J. Fluid Mech. (1982), *vol.* 116, *pp.* 363–378
Printed in Great Britain

Double-diffusive convection in an inclined fluid layer

By SIVAGNANAM THANGAM,† ABDELFATTAH ZEBIB AND C. F. CHEN‡

Department of Mechanical and Aerospace Engineering,
Rutgers University, New Brunswick, NJ 08903, U.S.A.

(Received 30 July 1980 and in revised form 14 July 1981)

The nonlinear double-diffusive convection in a Boussinesq fluid with stable constant vertical solute gradient, and bound by two differentially heated rigid inclined parallel plates is considered. The analysis was carried out by a Galerkin method for the cases when the angle of inclination was 0°, −45° and +45° (positive angle denotes heating from below, and negative angle denotes heating from above). The counter-rotating cells predicted by the linear theory merge into single cells with the same sense of rotation within a very short period of time even under slightly supercritical conditions. This is consistent with the experimental observations. Furthermore, as observed in the experiments, the evolution of instability is more rapid when heating is from above than when heating is from below. Our results for a salt–heat system are in excellent agreement with those based on the limiting case of Lewis number → 0 and Schmidt number → ∞.

1. Introduction

We consider the case of an inclined fluid layer with a stable constant solute gradient in the vertical direction and bound by two differentially heated, infinitely long parallel plates. The plates are assumed to be perfectly conducting to heat and non-diffusive to the solute. If the heating is slow, the temperature gradient across the layer would be constant and, under these conditions, a steady stable motion exists within the slot. While the buoyancy forces dominate near the boundaries, there may be no net density gradient in the interior region. However, any lateral displacement of the fluid could result in destabilization, since the diffusivities of heat and solute are considerably different, thus causing the two components to equilibrate at different rates. Experimental and theoretical investigations for this problem were carried out by Paliwal & Chen (1980*a*, *b*). Their results show that the agreement between the theoretical predictions based on a linear stability analysis and the experimental observations of the critical parameters is very good. However, while the linear stability analysis predicts the formation of pairs of counter-rotating cells at the onset of the instability (Paliwal 1979), the experimental observations indicate that the instability manifests itself in the form of two-dimensional convection rolls with the same sense of rotation (i.e. with the fluid rising near the hot wall and sinking near the cold wall).

The aim of the present analysis is to study the evolution of the flow after the onset

† Present address: Stevens Institute of Technology, Hoboken, NJ 07030, U.S.A.
‡ Present address: The University of Arizona, Tucson, Arizona 85721, U.S.A.

of instability, and to investigate whether the inclusion of the nonlinear terms in the governing equations could generate a flow pattern that would closely resemble that observed in the experiments. Hart (1973) has considered the nonlinear problem of a vertically stratified fluid subjected to differential heating in a vertical slot. His results indicated that, with the inclusion of nonlinear terms in the governing equations, the streamline pattern predicted by the linear theory could be altered considerably. The analysis was carried out by a finite-amplitude method based on weak nonlinear interaction theory. In order to facilitate algebraic simplicity, he used the flow parameters describing the asymptotic stable steady state corresponding to the case of large solute Rayleigh number (defined in § 2). Reddy (1980) solved the full nonlinear system of governing equations describing the motion in a vertical slot, using a finite-difference method with some approximations. Owing to numerical difficulties, the computations were restricted to the cases of only moderate values of solute Rayleigh number, and for lateral boundaries that were diffusive to both heat and solute. To simplify the analysis further, the stable steady state was assumed to be quiescent with no net horizontal density gradients. His results indicate that, to a certain extent, qualitative agreement with the experimental observations of Wirtz & Reddy (1979) could be obtained.

We have solved the full nonlinear system of governing equations describing the double-diffusive motion in an inclined slot by a Galerkin method. To keep the analysis as general as possible, no approximations have been made, either in the equations describing the stable steady motion, or in the boundary conditions. In order to obtain comparison with the experimental observations of Paliwal & Chen (1980*a*), the computations were done with the values of the flow parameters used in their experiments. In addition, since the diffusivity of heat is much larger than that of the solute, computations based on an asymptotic approximation as suggested by Straus (1972) were also carried out.

2. Formulation

An inclined fluid layer bound by two rigid parallel plates is considered. The coordinate system is shown in figure 1. There is a constant stable solute gradient $\Phi_0^* = dS_0^*/d\zeta$ (< 0) in the vertical direction. The plates are infinitely long in the z-direction and are inclined at an angle ϕ from the vertical. It is assumed that the plates are perfect heat conductors, maintained at a temperature of ΔT^*. The isosolutal lines are parallel with an upward tilt towards the hot wall everywhere except near the walls, where they become normal to the walls due to the non-diffusive boundary conditions. For small variations in salinity and temperature, the equation of state could be written as

$$\rho^* = \rho_r^*\{1 - \beta_t^*(T^* - T_r^*) + \beta_s^*(S^* - S_r^*)\}, \tag{2.1}$$

where

$$\beta_s^* = -\frac{1}{\rho_r^*}\left(\frac{\partial \rho^*}{\partial S^*}\right)_{T^*, P^*}, \quad \beta_t^* = -\frac{1}{\rho_r^*}\left(\frac{\partial \rho^*}{\partial T^*}\right)_{S^*, P^*}.$$

The subscript r indicates a suitable reference state and the superscript $*$ indicates that the quantities are in dimensional form. T, S, P and ρ indicate respectively temperature, salinity, pressure and density.

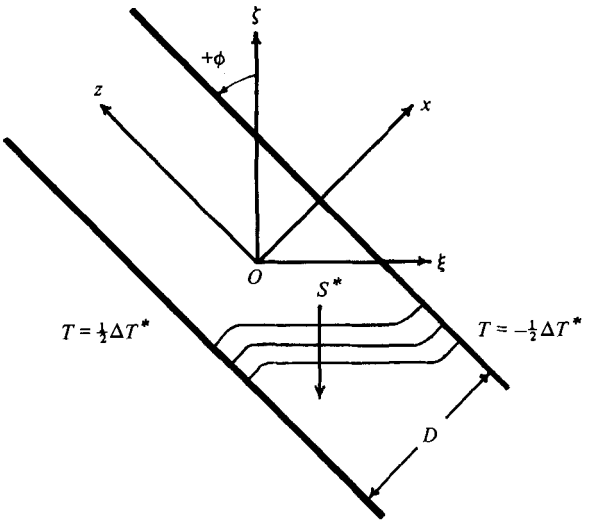

FIGURE 1. The co-ordinate system.

The equation of motion for this system could now be made dimensionless with the following scaling parameters: D for length, D^2/κ_s for time, $L\Delta T^*$ for temperature, and $D|\Phi_0^*|$ for the solute. The two-dimensional equations of motion in the (x,z)-plane with the Boussinesq approximation could then be written as

$$\left[\frac{1}{Sc}(\partial_\tau - \Psi_z\partial_x + \Psi_x\partial_z) - (\partial_{xx}+\partial_{zz})\right](\partial_{xx}+\partial_{zz})\Psi + \left(R_t T_z - \frac{R_s}{L}S_z\right)\sin\phi - \left(R_t T_x - \frac{R_s}{L}S_x\right)\cos\phi = 0, \quad (2.2)$$

$$[L(\partial_\tau - \Psi_z\partial_x + \Psi_x\partial_z) - (\partial_{xx}+\partial_{zz})]T = 0, \quad (2.3)$$

$$[(\partial_\tau - \Psi_z\partial_x + \Psi_x\partial_z) - (\partial_{xx}+\partial_{zz})]S = 0, \quad (2.4)$$

where $R_t = g\beta_t^*\Delta T^* D^3/\kappa_t\nu$ is the thermal Rayleigh number, $R_s = g\beta_s^*|\Phi_0^*|D^4/\kappa_t\nu$ is the solute Rayleigh number, $Sc = \nu/\kappa_s$ is the Schmidt number, and $L = \kappa_s/\kappa_t$ is the Lewis number. Here, the partial derivatives are represented by subscripts.

The stream function Ψ is defined such that $u = -\Psi_z$, and $w = \Psi_x$, and the boundary conditions are

$$\Psi = \Psi_x = 0, \quad S_x = 0, \quad T = \pm(2L)^{-1} \quad \text{at} \quad x = \mp\tfrac{1}{2}. \quad (2.5)$$

In the stable steady state, the flow is parallel to the side walls. Equations (2.2)–(2.4) together with boundary conditions (2.5) simplify to a linear, fourth-order ordinary differential equation for the vertical component of velocity, which can be readily solved. The solutions are given by Paliwal & Chen (1980*b*). It should be noted, however, that their solutions are presented in a slightly different set of non-dimensional parameters.

When each of the variables Ψ, T and S in (2.2)–(2.4) are expressed as a sum of the

mean and the perturbation quantity, the following set of perturbation equations are obtained:

$$\nabla^2\psi_\tau = Sc\left[\nabla^4\psi + \frac{1}{Sc}(W_{0_{xx}}\psi_z - W_0\psi_{zzz} - W_0\psi_{zxx}) + \cos\phi\left(R_t\theta_x - \frac{R_s}{L}s_x\right) - \sin\phi\left(R_t\theta_z - \frac{R_s}{L}s_z\right)\right] + \psi_z\psi_{zzx} + \psi_z\psi_{xxx} - \psi_x\psi_{zzz} - \psi_x\psi_{zxx}, \tag{2.6}$$

$$\theta_\tau = \frac{1}{L}\nabla^2\theta - W_0\theta_z + T_{0_x}\psi_z + \psi_z\theta_x - \psi_x\theta_z, \tag{2.7}$$

$$s_\tau = \nabla^2 s - W_0 s_z + S_{0_x}\psi_z - S_{0_z}\psi_x + \psi_z s_x - \psi_x s_z, \tag{2.8}$$

where $\nabla^2 = \partial_{xx} + \partial_{zz}$, $\psi = \Psi - \Psi_0$, $\theta = T - T_0$, and $s = S - S_0$. The subscript 0 denotes steady-state quantities. Based on the experimental observations of Paliwal & Chen (1980*a*), we assume that the perturbations are periodic in z. The boundary conditions are

$$\left.\begin{aligned}\psi = \psi_x = \theta = s_x = 0 \quad \text{at} \quad x = \pm\tfrac{1}{2},\\ \{\psi, \theta, s\}_{z=0} = \{\psi, \theta, s\}_{z=\pm j\lambda},\end{aligned}\right\} \tag{2.9}$$

where j is any positive integer between 0 and ∞, and the wavelength $\lambda = 2\pi/\alpha$, with α the wavenumber.

3. Method of solution

A Galerkin method is employed to solve the system of equations (2.6)–(2.9). We expand the variables ψ, θ and s in a double series in x and z, in terms of complete sets of orthogonal functions that satisfy the homogeneous, and the periodicity boundary conditions (2.9):

$$\psi = \sum_{k,l} a_{kl}(\tau)\,\psi_k(x)\,e^{il\alpha z}, \tag{3.1}$$

$$\theta = \sum_{k,l} b_{kl}(\tau)\,\theta_k(x)\,e^{il\alpha z}, \tag{3.2}$$

$$s = \sum_{k,l} c_{kl}(\tau)\,s_k(x)\,e^{il\alpha z}, \tag{3.3}$$

where $1 \leqslant k < \infty$, $-\infty < l < \infty$, $a_{k,l} = \tilde{a}_{k,-l}$, $b_{kl} = \tilde{b}_{k,-l}$ and $c_{kl} = \tilde{c}_{k,-l}$, with $\sim$ denoting the complex conjugate.

The functions $\psi_k(x)$ and $\theta_k(x)$ are the same as those first proposed by Chandrasekhar (1961) for solving thermal-convection problems and were later used by Busse (1967) for solving nonlinear thermal-convection problems. The function $s_k(x)$ is the same as that used by Paliwal & Chen (1980*b*). When the expansions for ψ, θ and s from (3.1)–(3.3) are substituted into (2.6)–(2.8) and the resulting formal expressions are made orthogonal to the expansion functions themselves, a system of first-order nonlinear equations describing the evolution of coefficients a_{kl}, b_{kl} and c_{kl} with time are obtained:

$$\dot{a}_{rq} = -Sc\sum_p G_{pr}\Bigg\{\sum_k\Bigg\{[q^4\alpha^4\delta_{kp} + 2q^2\alpha^2(\psi_k,\psi_p) + (\psi_k'',\psi_p'')]$$
$$+\frac{iq\alpha}{Sc}(W_{0_{xx}},\psi_k,\psi_p) + q^2\alpha^2(W_0,\psi_k,\psi_p) - (W_0,\psi_k,\psi_p)\Bigg\}\Bigg\}a_{kq}$$
$$+\sum_k R_t[\cos\phi(\theta_k',\psi_p) - iq\alpha\sin\phi(\theta_k,\psi_p)]\,b_{kq}$$
$$+\sum_k\frac{R_s}{L}[\cos\phi(s_k',\psi_p) - iq\alpha\sin\phi(s_k,\psi_p)]\,c_{kq}$$
$$+i\alpha\sum_p G_{pr}\sum_{k,m}\Bigg\{\sum_{l=1}^{\infty}\{(\psi_m,\psi_k'',\psi_p')[(q+l)\,\tilde{a}_{kl}\,a_{m(l+q)} - la_{k(l+q)}\tilde{a}_{ml}]$$
$$+(\psi_m',\psi_k'',\psi_p)[q\tilde{a}_{kl}\,a_{m(l+q)} + qa_{k(l+q)}\,a_{ml}]$$
$$+(\psi_m,\psi_k',\psi_p)[\alpha^2l^2q\tilde{a}_{kl}\,a_{m(l+q)} + \alpha^2(l+q)^2qa_{k(l+q)}\tilde{a}_{ml}]$$
$$+(\psi_m,\psi_k,\psi_p')[\alpha^2(l+q)^3\,a_{k(l+q)}\tilde{a}_{ml} - \alpha^2l^3\tilde{a}_{kl}\,a_{m(l+q)}]\}$$
$$+\sum_{l=0}^{q}[(\psi_m,\psi_k'',\psi_p')(q-l)\,a_{kl}\,a_{m(q-l)} + (\psi_m',\psi_k'',\psi_p)\,qa_{kl}\,a_{m(q-l)}$$
$$+(\psi_m,\psi_k',\psi_p)\,q\alpha^2l^2a_{kl}\,a_{m(q-l)} + (\psi_m,\psi_k,\psi_p')\,\alpha^2l^3a_{kl}\,a_{m(q-l)}]\Bigg\} \tag{3.4}$$

with $r \geqslant 1$, $q \geqslant 0$. Here, and in the following,

$$(F_k, F_p) = \int_{-\frac{1}{2}}^{\frac{1}{2}} F_kF_p\,dx \quad \text{etc.}$$

G_{pr}^q is the inverse of

$$A_{kp}^q = [q^2\alpha^2\delta_{kp} + (\psi_k',\psi_p')];$$

$$\dot{b}_{pq} = -\sum_k\left[\frac{1}{L}(q^2\alpha^2 + k^2\pi^2)\,\delta_{kp} + 2i\alpha q(W_0,\theta_k,\theta_p)\right]b_{kq} - \frac{2i\alpha q}{L}\sum_k(\psi_k,\theta_p)\,a_{kq}$$
$$+2i\alpha\sum_{m,k}\Bigg\{\sum_{l=1}^{\infty}[(\psi_m,\theta_k',\theta_p)[q\tilde{b}_{kl}\,a_{m(l+q)} + qb_{k(l+q)}\,a_{ml}]$$
$$+(\psi_m,\theta_k,\theta_p')[(l+q)\,b_{k(l+q)}\tilde{a}_{ml} - l\tilde{b}_{kl}a_{m(l+q)}]\}$$
$$+\sum_{l=0}^{q}[(\psi_m,\theta_k',\theta_p)\,qb_{kl}a_{m(q-l)} + (\psi_m,\theta_k,\theta_p')\,lb_{kl}a_{m(q-l)}]\Bigg\}, \tag{3.5}$$

$$\dot{c}_{pq} = -\frac{2}{\delta_{p1}+1}\sum_k\{[\tfrac{1}{2}q^2\alpha^2(\delta_{k1}+1) + \tfrac{1}{2}(k-1)^2\pi^2]\,\delta_{kp} + iq\alpha(W_0,s_k,s_p)\}c_{kq}$$
$$+\frac{2}{\delta_{p1}+1}\sum_k[iq\alpha(S_{0_x},\psi_k,s_p) + \cos\phi(\psi_k',s_p)]\,a_{kq}$$
$$+\frac{2i\alpha}{\delta_{p1}+1}\sum_{m,k}\Bigg\{\sum_{l=1}^{\infty}[(\psi_m,s_k',s_p)[q\tilde{c}_{kl}a_{m(l+q)} + qc_{k(l+q)}\tilde{a}_{ml}]$$
$$+(\psi_m,s_k,s_p')[(l+q)\,c_{k(l+q)}\tilde{a}_{ml} - l\tilde{c}_{kl}a_{m(l+q)})]$$
$$+\sum_{l=0}^{q}[(\psi_m,s_k',s_p)\,qc_{kl}\,a_{m(q-l)} + (\psi_m,s_k,s_p')\,lc_{kl}\,a_{m(q-l)}]\Bigg\}. \tag{3.6}$$

This system of nonlinear ordinary differential equations is solved numerically by the algorithm proposed by Gear (1971), with the initial conditions obtained from the eigenvectors of the linear stability problem (see appendix). Details of the calculation can be found in Thangam (1980).

4. Results and discussion

Before the results are analysed, a discussion on the numerical convergence of the results, and the influence of the initial conditions on the final solution is in order. To evaluate the numerical convergence, the changes in the kinetic energy and the Nusselt number of the system with time are studied during the evolution of instability. The kinetic energy K and Nusselt number N are defined as follows:

$$K = \frac{1}{2K_1}\int_0^{\lambda}\int_{-\frac{1}{2}}^{\frac{1}{2}} (\psi_x^2 + \psi_z^2)\,dx\,dz$$

$$= \frac{\pi}{K_1\alpha}\sum_{k,m,l}[(\psi_k', \psi_m') + l^2\alpha^2\delta_{km}](a_{kl}\tilde{a}_{ml} + \tilde{a}_{kl}a_{ml}); \tag{4.1}$$

where K_1 is the initial kinetic energy at time $\tau = 0$;

$$N = \{N\}_{\text{hot wall}} = \left[\left\langle 1 + \frac{\theta_x}{T_{0_x}}\right\rangle\right]_{\text{hot wall}}$$

$$= 1 - L\left[\sum_{k=\text{odd}} b_{k0}k\pi(-1)^{\frac{1}{2}(k-1)} + \sum_{k=\text{even}} b_{k0}k\pi(-1)^{\frac{1}{2}k}\right]. \tag{4.2}$$

Here, $k, m \geqslant 1$, $l \geqslant 0$ and the bracket $\langle\ \rangle$ indicates that the values inside are averaged over one wavelength in the z-direction. The number of terms in either the z-expansion or in the x-expansion is increased, and the changes in the kinetic energy and the Nusselt number at different time levels are compared until there is no appreciable difference in the computed values as a result of this increase. It was found that three terms in the z-expansion were sufficient for all angles of inclination. However, in the x-expansion, the number of terms required to achieve satisfactory convergence varied with the angle of inclination. At $\phi = 0°$, six terms were sufficient, but, at $\phi = 45°$, ten terms, and, at $\phi = -45°$, twelve terms were needed. It should be mentioned here that for $\phi = \pm 45°$, even after satisfactory convergence was achieved in both kinetic energy and Nusselt number, a certain amount of waviness in the x-direction was exhibited by the isovorticity lines (cf. figures 7 and 8). However, this wavy structure disappeared with further increase in the number of terms in the x-expansion. In the present investigation, the lower number of terms were used, mainly to reduce the computation time.

The initial conditions used to solve (3.4)–(3.6) are obtained from the eigenvector of the linear eigenvalue problem (see appendix). Thus the terms corresponding to the linear mode alone are present initially. It would then be interesting to see how the other modes grow with time. The distribution of kinetic energy in all these modes, and the growth of each mode are shown separately in figure 2, for the case of the vertical slot. Eight terms were used in the x-expansion, and R_t was kept at approximately 55 % above the critical value R_{tc}. The contributions to the net kinetic energy from modes higher than the second were almost negligible in magnitude. The results show clearly that the major contribution to the total kinetic energy comes from the fundamental, and the zero mode only.

To study the influence of initial conditions over the final solution, first the value of R_t was maintained constant and the kinetic energy of the initial disturbances were changed. When the value of R_t was maintained at 5 % above that of R_{tc}, the growth

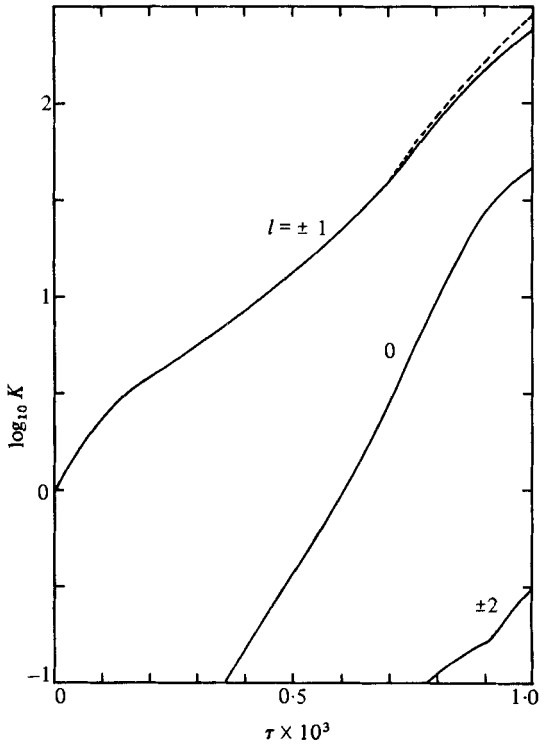

FIGURE 2. The spectral growth of kinetic energy with time. – – –, total kinetic energy; ——, spectral distribution of kinetic energy in z, lth component. $\phi = 0°$, $\alpha = 22{\cdot}5$, $R_s = 362000$, $R_t = 200000$, 8 terms in x.

in kinetic energy and Nusselt number were monitored at two different values of the initial kinetic energy, with the larger value being 2·5 times the smaller one. The results show that the growth in the kinetic energy and Nusselt number are more rapid when the input kinetic energy is larger at all three angles of inclination (see figures 3 and 4). In addition, when the initial value of the kinetic energy is held constant, the higher the value of the thermal Rayleigh number R_t above the critical value, the faster is the growth of the kinetic energy and the Nusselt number, as shown in figure 5. Hence, in order to compare the evolution of motion at different angles of inclination, the input kinetic energy and the ratio of R_t over the critical value R_{tc} need to be maintained at the same level.

In this analysis the wavenumber was maintained at the critical value (cf. table 1), and the values of R_s, Sc and L corresponding to the experimental values of Paliwal & Chen (1980*a*) were used (i.e. $R_s = 3{\cdot}62 \times 10^5$, $Sc = 556$, $L = 0{\cdot}012$, with the scaling factors $D = 1$ cm, $D^2/\kappa_s = 5{\cdot}5 \times 10^4$ s, and $|\phi_0^*| = 5{\cdot}2 \times 10^{-3}$ cm^{-1}). The computations were carried out at the angles of inclination $\phi = 0°$, $+45°$ and $-45°$ and, for all three cases under consideration, the thermal Rayleigh number R_t was maintained at 5 % above the corresponding critical value. The results shown in figures 6–8 consist of the plots of the streamlines ψ, isovorticity lines ω, isotherms T, and isosolutal lines S, at different time intervals. In each plot, the isopleths are divided into equal intervals of DELF between the maximum value, FMAX, and the minimum value, FMIN. The section of the plot shown has the x-co-ordinate in the horizontal direction, with the

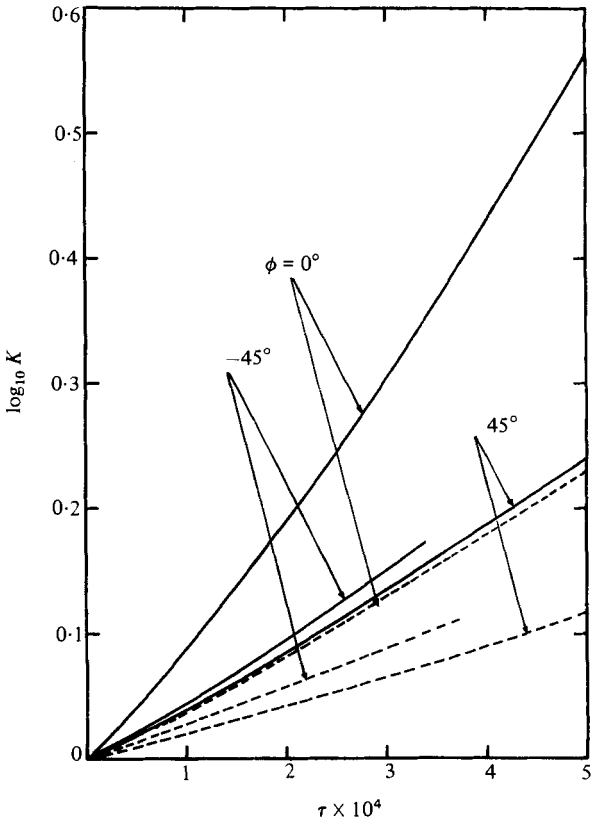

FIGURE 3. The effect of change in the initial kinetic energy on the growth of kinetic energy with time at various values of the angle of inclination. $R_i = 1{\cdot}05R_{ic}$ and $\alpha = \alpha_c$. Initial K (——) = 2·5 × initial K (– – –).

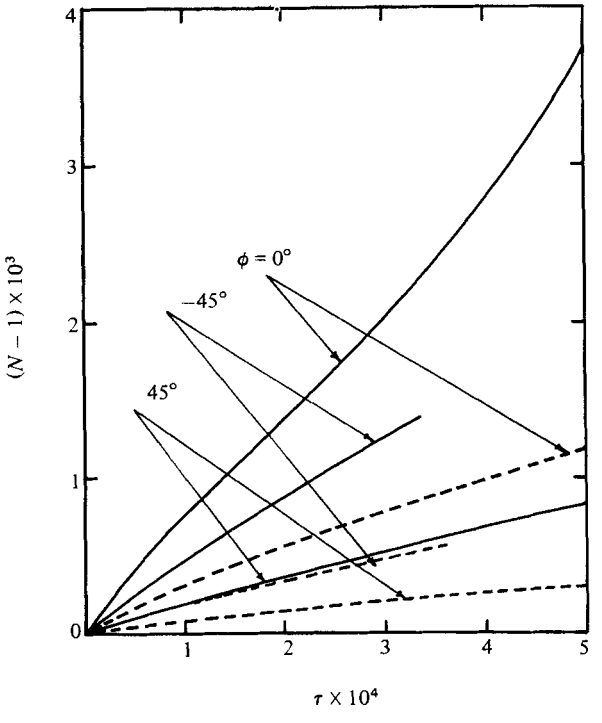

FIGURE 4. The effect of change in the initial kinetic energy on the growth of Nusselt number with time at various values of the angle of inclination. Other details are the same as in figure 3.

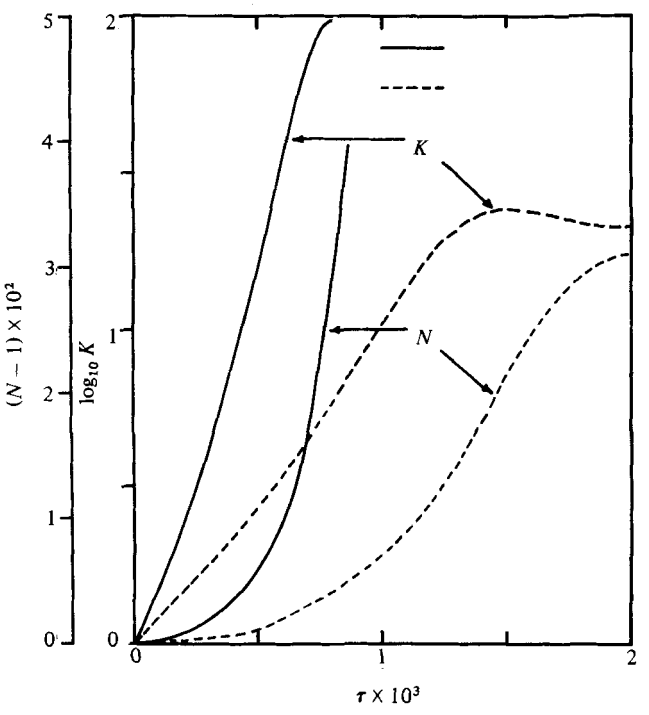

FIGURE 5. The effect of change in thermal Rayleigh number on the growth of the kinetic energy and Nusselt number. ——, $R_t = 1{\cdot}50R_{tc}$; – – –, $R_t = 1{\cdot}05R_{tc}$. $\phi = 0°$, $\alpha = 22{\cdot}5$, $R_s = 362000$, 6 terms in x, 3 terms in z.

Angle	R_{tc}	α_c
0°	125710	22·5
−45°	128570	16·5
+45°	167620	12·9

TABLE 1. Results from linear stability analysis; $R_s = 362000$, $Sc = 556$, $L = 0{\cdot}012$

value of x ranging from $-0{\cdot}5$ to $+0{\cdot}5$, and the z-co-ordinate in the vertical direction, with the value of z ranging from 0 to 2λ. Thus, for the case of the streamlines and the isovorticity lines, there are two cells in each plot. In figure 6 and 7, the hot wall is at the left-hand side (i.e. at $x = -0{\cdot}5$) and, in figure 8, the hot wall is at the right-hand side (i.e. at $x = 0{\cdot}5$). The cells in all these cases tilt up towards the hot wall. From the results, it can be seen that the pairs of counter-rotating cells predicted by the linear theory (Paliwal & Chen 1980*b*), merge into cells with the same sense of rotation, i.e. with the fluid rising near the hot wall and sinking near the cold wall. The predicted upward tilt of these cells compare favourably with the disposition of cells shown in shadowgraphs obtained by Paliwal & Chen (1980*a*) for all three angles. In both figures 7 and 8, the isovorticity lines show a certain amount of waviness in the x-direction. These will disappear as the number of terms in the x-expansion are increased as discussed previously. Though the merging takes place in a short time, $\sim$ 1 s, consistent with the experimental results in all these cases, the magnitude and

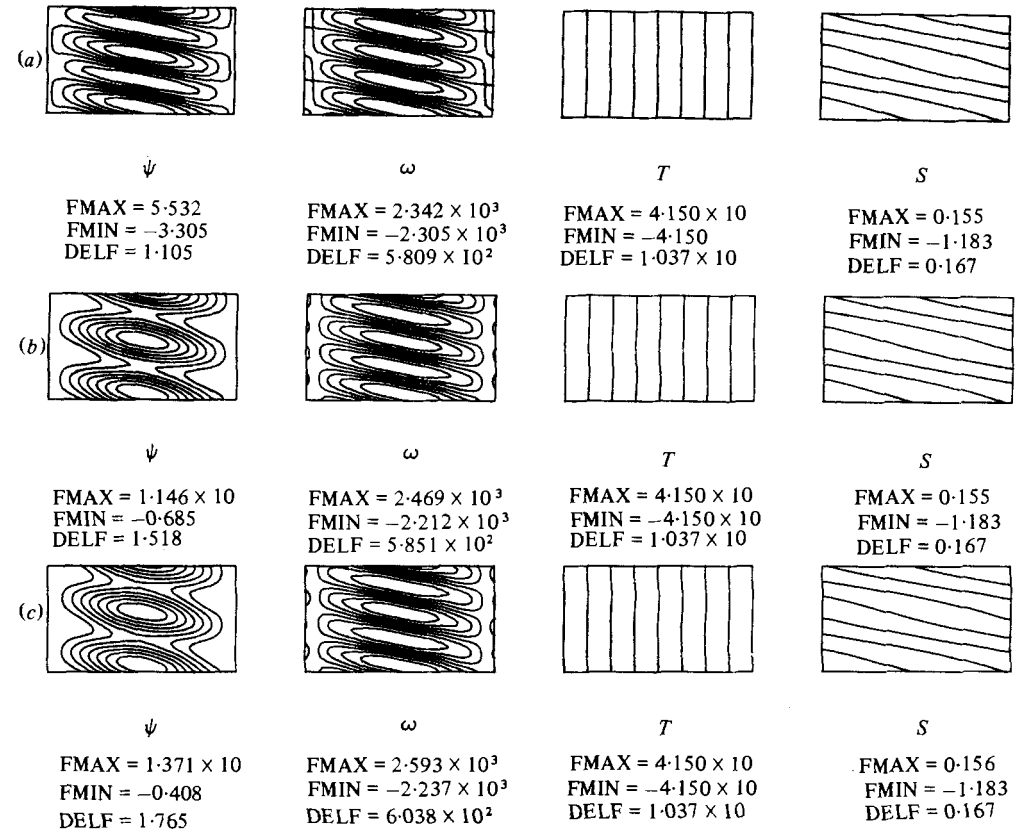

FIGURE 6. The evolution of instability in a vertical slot, $\phi = 0°$; contours of streamlines ψ, isovorticity lines ω, isotherms T and isosolutal lines S. $R_s = 362000$, $R_t = 132000$, $L = 0{\cdot}012$, $Sc = 556$ and $\alpha = 22{\cdot}5$. (*a*) Time $= 0{\cdot}5 \times 10^{-5}$; (*b*) $1{\cdot}5 \times 10^{-5}$; (*c*) $3{\cdot}0 \times 10^{-5}$.

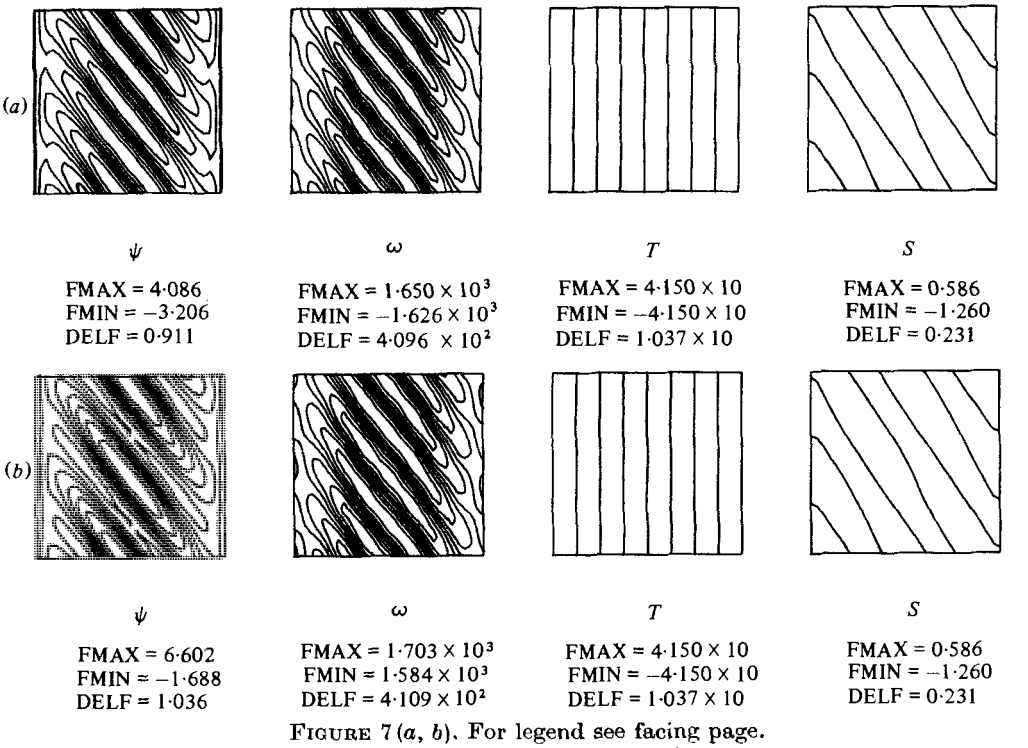

FIGURE 7 (*a*, *b*). For legend see facing page.

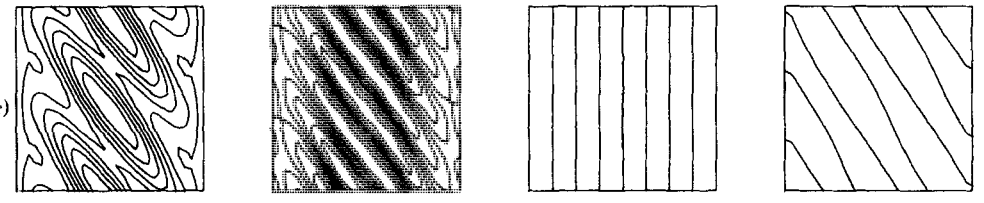

(c)

ψ	ω	T	S
FMAX = 1·025 × 10	FMAX = 1·784 × 10^3	FMAX = 4·150 × 10	FMAX = 0·586
FMIN = −1·688	FMIN = −1·539 × 10^3	FMIN = −4·150 × 10	FMIN = −1·260
DELF = 1·492	DELF = 4·154 × 10^2	DELF = 1·037 × 10	DELF = 0·231

FIGURE 7. The evolution of instability in an inclined slot, $\phi = +45°$. Contours of streamlines ψ, isovorticity lines ω, isotherms T and isosolutal lines S. $R_s = 362000$, $R_t = 176000$, $L = 0{\cdot}012$, $Sc = 556$ and $\alpha = 12{\cdot}9$. (*a*) Time = $0{\cdot}5 \times 10^{-5}$; (*b*) $1{\cdot}5 \times 10^{-5}$; (*c*) $3{\cdot}0 \times 10^{-5}$.

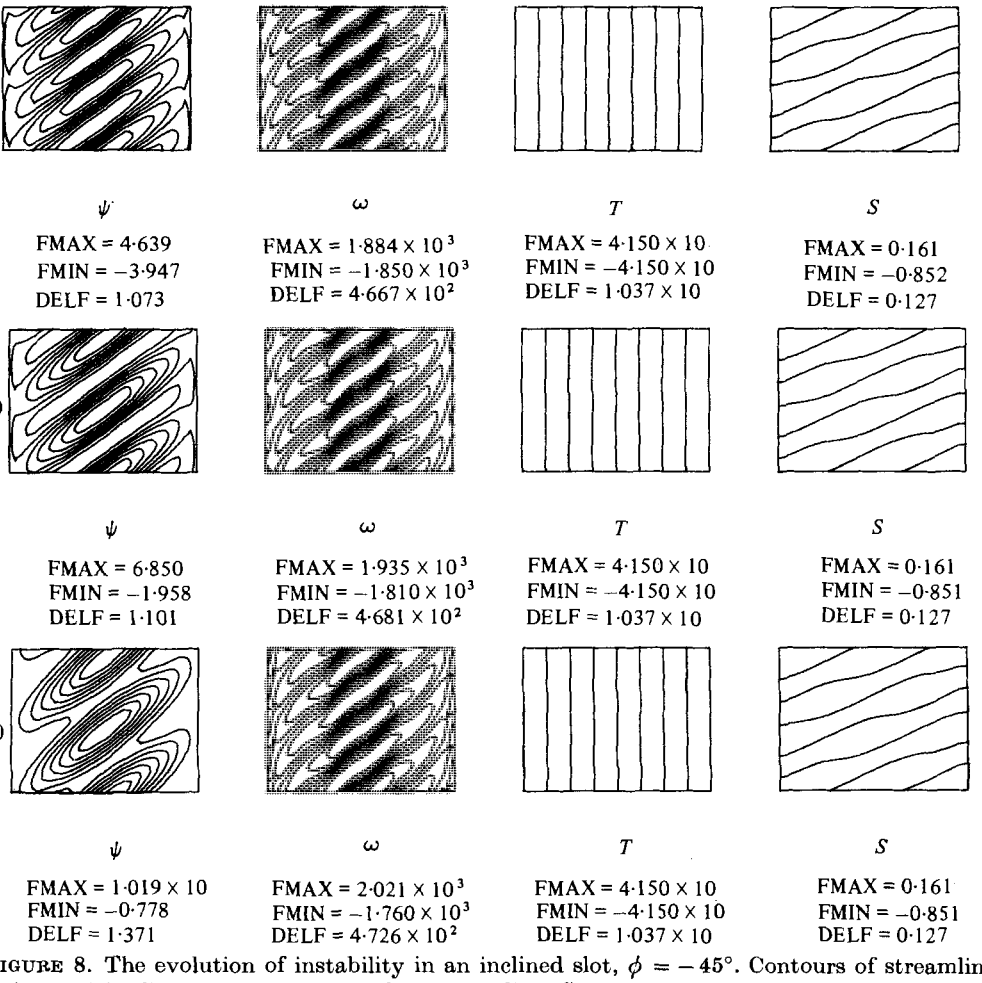

(a)

ψ	ω	T	S
FMAX = 4·639	FMAX = 1·884 × 10^3	FMAX = 4·150 × 10	FMAX = 0·161
FMIN = −3·947	FMIN = −1·850 × 10^3	FMIN = −4·150 × 10	FMIN = −0·852
DELF = 1·073	DELF = 4·667 × 10^2	DELF = 1·037 × 10	DELF = 0·127

(b)

ψ	ω	T	S
FMAX = 6·850	FMAX = 1·935 × 10^3	FMAX = 4·150 × 10	FMAX = 0·161
FMIN = −1·958	FMIN = −1·810 × 10^3	FMIN = −4·150 × 10	FMIN = −0·851
DELF = 1·101	DELF = 4·681 × 10^2	DELF = 1·037 × 10	DELF = 0·127

(c)

ψ	ω	T	S
FMAX = 1·019 × 10	FMAX = 2·021 × 10^3	FMAX = 4·150 × 10	FMAX = 0·161
FMIN = −0·778	FMIN = −1·760 × 10^3	FMIN = −4·150 × 10	FMIN = −0·851
DELF = 1·371	DELF = 4·726 × 10^2	DELF = 1·037 × 10	DELF = 0·127

FIGURE 8. The evolution of instability in an inclined slot, $\phi = -45°$. Contours of streamlines ψ, isovorticity lines ω, isotherms T and isosolutal lines S. $R_s = 326000$, $R_t = 135000$, $L = 0{\cdot}012$, $Sc = 556$ and $\alpha = 16{\cdot}5$. (*a*) Time = $0{\cdot}5 \times 10^{-5}$; (*b*) $1{\cdot}5 \times 10^{-5}$; (*c*) $3{\cdot}0 \times 10^{-5}$.

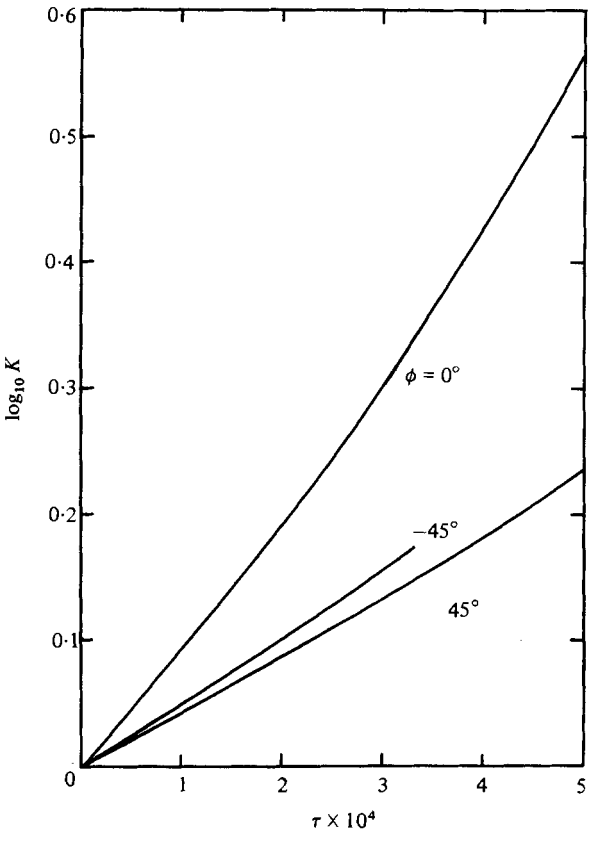

FIGURE 9. The growth in kinetic energy with time. $R_t = 1{\cdot}05\, R_{tc}$ and $\alpha = \alpha_c$.

the shape of the streamlines and the isovorticity lines are not the same at different angles of inclination. In addition, there are differences in the structure and the shape of the isotherms and the isosolutal lines.

Thus, in order to obtain a better understanding of the evolution of motion at different angles of inclination, the growth in kinetic energy with time is considered. The results as shown in figure 9 indicate that the growth is more rapid when heating is from above than when heating is from below, and that this growth of kinetic energy with time is most rapid in the vertical fluid layer. In figure 10, the variation of Nusselt number at the hot wall with time is shown. The trend in the growth of the Nusselt number is similar to that of the kinetic energy, and the results again show that the evolution of instability is faster when heating is from above, compared to the case when heating is from below. This finding offers theoretical confirmation to the experimental observations made by Paliwal & Chen (1980*a*), and can be explained by the vertical salinity distribution in these two cases.

The results also show that the growth of disturbances is most rapid in a vertical slot. This may be explained by the fact that, the higher the temperature gradient in the horizontal direction, the faster the evolution of the instability. For the same lateral temperature difference, the temperature gradient in the horizontal direction for the vertical fluid layer is larger than that in inclined fluid layers. Based on this consideration alone, the vertical fluid layer would be the most unstable. Hence, to compare the

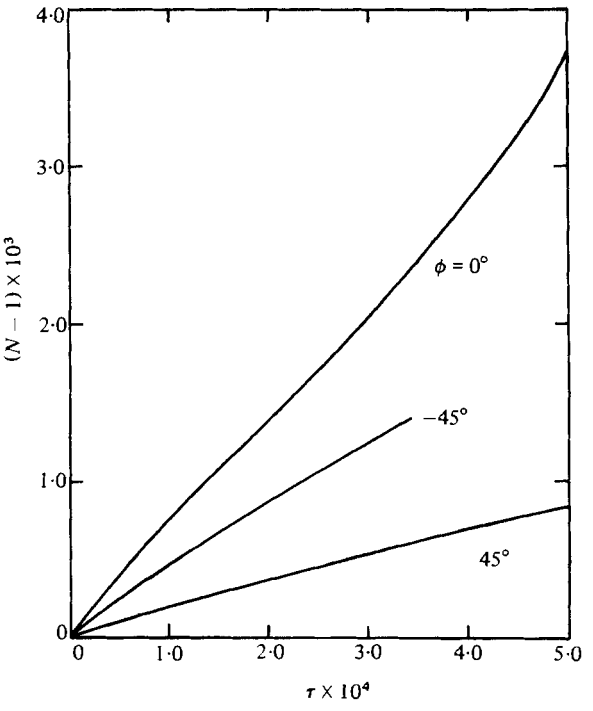

FIGURE 10. The growth in Nusselt number with time. Other details are the same as in figure 9.

stability of an inclined fluid layer heated from above with that of a vertical fluid layer heated from its side, the relative magnitudes of the horizontal and the vertical density gradients should be considered. The experimental and theoretical results based on a linear stability analysis of Paliwal & Chen (1980*a*, *b*) show that, up to moderately small angles of inclination, the vertical fluid layer is more stable when compared to the inclined fluid layer heated from above; while, at larger angles of inclination, the inclined layer heated from above is stabler.

5. A limiting case: $L \to 0$ and $Sc \to \infty$

We consider the following limiting case (cf. Straus 1972) in which the thermal diffusivity and the kinematic viscosity are much larger than the solute diffusivity. The heat–salt system is a typical example; the Lewis number is $\sim 10^{-2}$ and the Schmidt number is $\sim 7 \times 10^2$. Thus, for this problem, the limiting case of $L \to 0$ and $Sc \to \infty$ can introduce considerable simplifications in (3.4)–(3.6). The momentum and the heat-transport equations reduce to a system of linear algebraic equations for the expansion coefficients. However, all the terms in the transport equation for solute are retained, and a system of coupled first-order nonlinear ordinary differential equations is obtained. The initial conditions are again obtained from the linear eigenvalue problem. The ordinary differential equations are first solved and the values of the coefficients for salinity at the next time-step are obtained (Gear 1971). These updated values are then used to solve the system of linear algebraic equations for the coefficients of stream function and temperature by a Gaussian elimination process using the Crout algorithm (Forsythe & Moler 1967). As anticipated, the results based on the

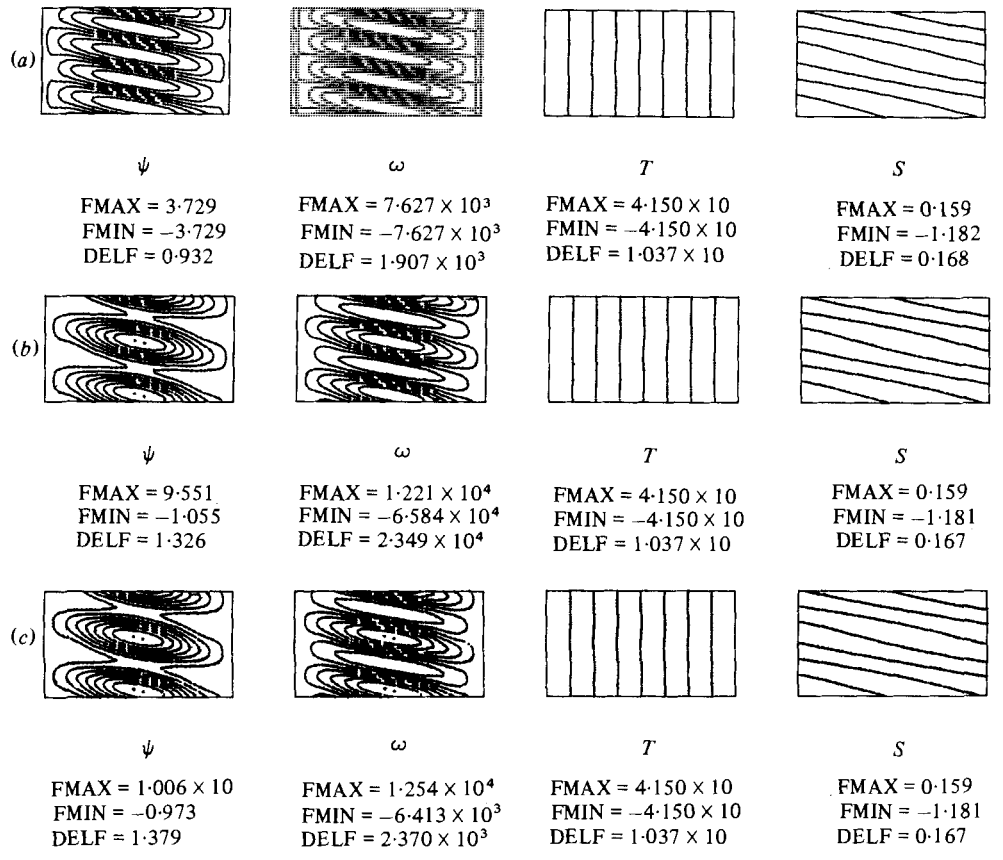

FIGURE 11. The evolution of instability in a vertical slot, $\phi = 0°$. Contours of streamlines ψ, isovorticity lines ω, isotherms T and isosolutal lines S, for the general and the limiting case. $R_s = 362000$, $R_t = 132000$ and $\alpha = 22{\cdot}5$. (*a*) Time = 0; (*b*) $2{\cdot}0 \times 10^{-4}$, $L = 0{\cdot}012$, $Sc = 556$; (*c*) $2{\cdot}0 \times 10^{-4}$, $L \to 0$, and $Sc \to \infty$.

limiting case $L \to 0$ and $Sc \to 0$ agreed well with the heat–salt case. For comparison, the plots of ψ, ω, T and S are given in figure 11 at some selected time levels for the cases with and without the limiting approximation. The plotting details for figure 11 are the same as that of figure 6. No attempt was made to plot the growth in kinetic energy with time for these two cases, as it was almost impossible to distinguish between the results. However, the Nusselt number N is always equal to unity for the case with the limiting approximation, unlike the case without such an approximation, where there is a net growth in N with time. The magnitude of this growth is small, and the results indicated in figure 11 confirm this fact. In fact, there is little difference in the temperature and the salinity profiles, while the differences in the streamlines and the isovorticity profiles are quite small.

6. Conclusions

A nonlinear analysis has been carried out to study the initial evolution of the double-diffusive instability in an inclined fluid layer. The pairs of counter-rotating cells predicted by the linear theory merge into single cells with the same sense of rotation as indicated by experiments, even under conditions that are only slightly supercritical,

within a very short period of time. The results indicate that the evolution of instability in an inclined fluid layer, stratified by solute distribution, is faster when heating is from above, compared with the case when the heating is from below. In addition, the results show that there is no observable steady state in the range of our computations.

The authors would like to acknowledge the financial support provided by the National Science Foundation through Grant ENG78-16962.

Appendix. Linear eigenvalue problem

The linearized perturbation equations are obtained by neglecting the nonlinear terms in (3.13)–(3.15). The expansion coefficients a_{1k}, b_{1k}, and c_{1k} are now assumed to be proportional to $\exp \sigma\tau$ and the resulting system of equations could be written as

$$(\mathbf{A}-\sigma\mathbf{I})\,\mathbf{x} = 0. \tag{A 1}$$

Here, the matrix $\mathbf{A}$ is complex, $\mathbf{I}$ represents the identity matrix, and the vector $\mathbf{x}$ contains the unknown coefficients a_{1k}, b_{1k} and c_{1k}. The eigenvalues of the system of (A 1) are first computed through the modified LR algorithm of Martin & Wilkinson (1968*a*, *b*). These eigenvalues σ are a function of the Lewis number L, the Schmidt number Sc, the solute Rayleigh number R_s, the angle of inclination ϕ, the wavenumber α, and the thermal Rayleigh number R_t. The neutral states of these parameters occur when the condition $\max[\mathscr{R}(\sigma)] = 0$ is satisfied. In the present analysis, the parameters L, Sc and R_s are kept constant at the values corresponding to those used by Paliwal & Chen (1980*a*). Then, for a given value of ϕ, the other two remaining parameters, α and R_t, are relaxed and the critical states are determined. The results for $\phi = 0°$, $45°$ and $-45°$ are given in table 1, and these are in agreement with those obtained by Paliwal & Chen (1980*b*). In order to obtain the appropriate initial conditions for the nonlinear problem, the value of the wavenumber α is maintained at its critical value, and the eigenvector of the linear problem is computed through the modified QR algorithm of Peters & Wilkinson (1970).

REFERENCES

Busse, F. H. 1967 On the stability of two-dimensional convection in a layer heated from below. *J. Math. & Phys.* **46**, 140–150.

Chandrasekhar, S. 1961 *Hydrodynamic and Hydromagnetic Stability*, pp. 633–637. Clarendon.

Forsythe, G. & Moler, C. B. 1967 *Computer Solution of Linear Algebraic Systems*. Prentice-Hall.

Gear, C. W. 1971 *Numerical Initial-Value Problems in Ordinary Differential Equations*. Prentice-Hall.

Hart, J. E. 1970 Thermal convection between sloping parallel boundaries. Ph.D. thesis, Massachusetts Institute of Technology.

Hart, J. E. 1973 Finite amplitude sideways diffusive convection. *J. Fluid Mech.* **59**, 47–64.

Martin, R. S. & Wilkinson, J. H. 1968*a* Similarity reduction of a general matrix to Hessenberg form. *Numer. Math.* **12**, 349–368.

Martin, R. S. & Wilkinson, J. H. 1968*b* The modified LR algorithm for complex Hessenberg matrices. *Numer. Math.* **12**, 369–376.

Paliwal, R. C. 1979 Double-diffusive convective stability in an inclined fluid layer. Ph.D. thesis, Rutgers University.

Paliwal, R. C. & Chen, C. F. 1980*a* Double-diffusive instability in an inclined fluid layer. Part 1. Experimental investigations. *J. Fluid Mech.* **98**, 755–768.

PALIWAL, R. C. & CHEN, C. F. 1980*b* Double-diffusive instability in an inclined fluid layer. Part 2. Theoretical investigations. *J. Fluid Mech.* **98**, 769–785.

PETERS, G. & WILKINSON, J. H. 1970 Eigenvectors of real and complex matrices by LR and QR triangularizations. *Numer. Math.* **16**, 181–204.

REDDY, C. S. 1980 Cell merging and its effect on heat transfer in thermosolutal convection. *J. Heat Transfer* **102**, 172–174.

STRAUS, J. M. 1972 Finite amplitude doubly diffusive convection. *J. Fluid Mech.* **56**, 353–374.

THANGAM, S. 1980 Experimental and theoretical investigations on the influence of shear in double-diffusive convection. Ph.D. thesis, Rutgers University.

WIRTZ, R. A. & REDDY, C. S. 1979 Experiments on convecting layer formation and merging in a differentially heated slot. *J. Fluid Mech.* **91**, 451–464.